



Application of Box-Behnken Method Based ANN-GA to Prediction of wt.% of Doping Elements for Incoloy 800H Coated by Aluminizing-Chromizing

Dr. Abbas Khammas Hussein

Assistant Professor

University of Technology, Department of Materials Engineering

Email: abbas2000x@yahoo.com

ABSTRACT

In this work, an effective procedure of Box-Behnken based-ANN (Artificial Neural Network) and GA (Genetic Algorithm) has been utilized for finding the optimum conditions of wt.% of doping elements (Ce, Y, and Ge) doped-aluminizing-chromizing of Incoloy 800H. ANN and Box-Behnken design method have been implanted for minimizing hot corrosion rate k_p ($10^{-12} \text{g}^2 \cdot \text{cm}^{-4} \cdot \text{s}^{-1}$) in Incoloy 800H at 900°C . ANN was used for estimating the predicted values of hot corrosion rate k_p ($10^{-12} \text{g}^2 \cdot \text{cm}^{-4} \cdot \text{s}^{-1}$). The optimal wt.% of doping elements combination to obtain minimum hot corrosion rate was calculated using genetic algorithm approach. The predicted optimal values for minimizing hot corrosion rate for Incoloy 800H coated by (Ce-Y-Ge) doped-aluminizing-chromizing are (3wt.%Ce, 3wt.%Y, and 3wt.%Ge), the hot corrosion rate k_p ($10^{-12} \text{g}^2 \cdot \text{cm}^{-4} \cdot \text{s}^{-1}$) value at these conditions was found to be 71.701. The results have been verified by confirmation experiment, results obtained by GA method match closely with experimental values ($R^2=98.30$). EDS and XRD results show that the formation of protective layers Al_2O_3 and Cr_2O_3 during hot corrosion tests.

Keywords: Box-behnken design, GA, ANN, Hot Corrosion, Pack cementation.

تطبيق طريقة بوكس-بينكن ذات أساس شبكات عصبونية إصطناعية-خوارزمية وراثية للتنبأ بالنسب الوزنية المثالية لعناصر الإضافة لسبيكة Incoloy 800H المغطاة بالألمنة-كرومنة

د.عباس خماس حسين

أستاذ مساعد

الجامعة التكنولوجية، قسم هندسة المواد

الخلاصة

يتضمن هذا البحث استخدام الأسلوب الفعال من خلال طريقة بوكس-بينكن ذات أساس شبكات عصبونية إصطناعية-خوارزمية وراثية لتحديد الظروف المثلى للنسب الوزنية لعناصر الإضافة (سيريوم-يتريوم-جرمانيوم) لعملية الألمنة-كرومنة لسبيكة Incoloy 800H. و استخدمت كل من طريقة التصميم بوكس-بينكن و الشبكات العصبونية لخفض معدل التآكل الساخن في سبيكة Incoloy 800H عند 900°C ، حيث استخدمت الشبكات العصبونية للتنبأ بقيم معدل التآكل الساخن، أما بالنسبة لمزيج النسب الوزنية المثالية لعناصر الإضافة اللازمة للحصول على القيمة الدنيا لمعدل التآكل الساخن فقد تم تحديدها بواسطة الخوارزمية الوراثة. و لوحظ أن القيم المثلى التي تم التنبأ بها لخفض معدل التآكل الساخن لسبيكة Incoloy 800H المغطاة بعناصر الإضافة (سيريوم-يتريوم-جرمانيوم) لعملية الألمنة-كرومنة هي (3wt.%Ce, 3wt.%Y, and 3wt.%Ge) أما قيمة معدل التآكل الساخن عند هذه الظروف فقد كانت $71.701 \times 10^{-12} \text{g}^2 \cdot \text{cm}^{-4} \cdot \text{s}^{-1}$. و قد تم التحقق من هذه الظروف من خلال تجربة التحقق (التأكد)، و لوحظ أن النتائج التي تم الحصول عليها من خلال طريقة الخوارزمية الوراثة تتطابق بشكل دقيق مع القيم التجريبية (معامل التحديد = 98.30). و أظهرت نتائج EDX و XRD تكون طبقات الحماية الأوكسيدية Al_2O_3 ، Cr_2O_3 خلال إختبارات التآكل الساخن.

الكلمات الرئيسية: تصميم وكس بينكن، الجينات الوراثة، الشبكات العصبونية، التآكل الساخن، تغليف السمنت.



1.INTRODUCTION

High-temperature oxidation, hot corrosion and erosion are the main failure modes of components in the hot sections of gas turbines, boilers, etc. Incoloy 800H have been developed for high temperature applications . This material finds application in the gas turbine industry, constituting over fifty percent of the gas turbine weight due to their good mechanical properties at high temperatures . In general, hot corrosion increases due to the transport in liquid phase of complex mixtures of molten sodium sulfate which cause catastrophic hot corrosion ., **Lin-Chang Tsai, et al., 2015, Fahamsyah H., et al, 2015, Subhash Kamal, et. al., 2015** . Hot corrosion refers to an accelerated corrosion, resulting from the presence of salt such as (Na_2SO_4), NaCl , V_2O_5 ...ect that combine to form molten deposits, which damage the protective surface oxides . This type of corrosion occurs when metals are subjected to the temperature range 700–900°C in the presence of sulphur deposits formed as a result of the reaction between sodium chloride and sulphur compounds in the presence of gas phase surrounding the metals .The Deposits of (Na_2SO_4) are molten at higher temperatures (m.p. 884°C) and can cause accelerated corrosion on Ni- and Co-based superalloys. This type of corrosion is commonly called ‘hot corrosion’., **Subhash Kamal, et al., 2010, T. S. Sidhu, et al., 2006** . Coating techniques play a important role in the operation at high temperatures, particularly for hot section parts, which are subjected to complex thermal and mechanical strain/stress cycling. Coatings are applied with a specific aim to improve the base material resistance by provide a barrier against high temperatures., **Marta Kianicova , et al., 2011, W.H Lee and R.Y Lin , 2003** . Pack cementation using aluminum, chromium or silicon is one of the easiest and cheapest processes to obtain the protective coatings to improve the corrosion resistance at high temperature ., **LIN Nai-ming, et al., 2010, Bruce M., et al., 2001**. The diffusion Coating method is used for surface alloying of protective coatings on the substrate surface, for example aluminizing, siliconizing, chromizing, simultaneous aluminizing-siliconizing, simultaneous aluminizing-siliconizing-chromizing and forms a thin oxide scale, which works as the diffusion barrier and reduces the oxidizing speed of the base material. , **A. ESLAMI, et al., 2009, I.M. Edmonds, et al., 2008, H. R. KARIMI ZARCHI, et al., 2013** . High temperature oxidation resistance is usually improved by the addition of some amount of oxygen reactive elements (doping elements) like Y and rare earth elements (REE) Ce, La, Er and others into surface metal. These elements is introduced through surface treatment techniques such as pack cementation. The incorporation *via* surface treatment acts in favour of doping elements concentration at the surface where the oxide will form and thus may have the most benefit, **Chao-Chi Jain and Chun-Hao Koo, 2007, Ranjan Sinha, et al., 2013, Hongyu Wang , et al., 2010**.

In this work, it has been reported the effects of amounts of oxygen reactive elements (Ce, Y, Ge) on the parabolic rate constant (Hot corrosion rate k_p ($10^{-12} \text{g}^2 \cdot \text{cm}^{-4} \cdot \text{s}^{-1}$)) through the hot corrosion experiment of Aluminized-Chromized Superfer 800H (Incoloy 800H) . Recently many statistical experimental design methods have been employed such Box-Behnken design . These methods involve mathematical models for designing which can be processed using Artificial Neural Network (ANN) and Genetic Algorithm (GA) . The main objective of (GA) is to determine the optimum operational conditions for the coating system .



2. MATERIALS AND COATING FORMULATIONS

The experimental work was performed by using samples of Superfer800H (Incoloy800). The spectrochemical analysis of candidate material is shown in Table 1. Samples were cut into squares shapes with dimensions of (10mm×10mm×4mm). All surfaces, including the edges were wet ground using 120, 220, 320, 600, 800, and 1200 grit silicon carbide papers. These samples were then cleaned with water, degreased with acetone, and then ultrasonically cleaned for 30 minutes using ethanol as a medium. After drying, the samples were stored in polyethylene zip-lock bags. The dimensions of all samples were measured. The pack mixture used for aluminum-chromium diffusion coating consisting of 20 Wt.%Al powder (40–45 μm in particule size) as an aluminum source, 10 Wt.%Cr powder (50-55 μm in particule size) as a chromium source, 2Wt.% NaF and 4Wt.%NaCl as activator and the balance was alumina-powder (80-110 μm in particule size). All pack powders were sized by sieving method and 1-3Wt.% of the pack alumina filler was replaced by reactive elements (Ce,Y,Ge) according to a standard response surface methodology (RSM) design called Box-Behnken Design (BBD). The samples was placed in a sealed stainless steel cylindrical retort of 50mm in a diameter and of 80mm in a height in contact with the pack mixture. The retort was then put in another stainless steel cylindrical retort of 80mm in a diameter and 140mm in a height. The outer retort has a side tube through which argon gas passes and second in the top cover for argon gas outlet. Type-k calibrated thermocouple was inserted through the cover of the outer retort for recording real temperature near inner retort. Figure 1 shows the apparatus used for pack cementation (University of Technology / Department of Production Engineering & Metallurgy). Pack cementation process was carried out at 1050 °C for 6 h under an Ar atmosphere according to **Robert A.Rapp et al procedure, 1991**. In order to examine the microstructure of the coatings before and after hot corrosion test at the optimum conditions, the coated and tested samples were mounted and ground up to 1000 grit with SiC paper and then polished using 1μm diamond paste. The samples were then analyzed using energy dispersive spectroscopy(EDS), x-ray diffraction (XRD), and optical microscope.

3. HOT CORROSION TEST

For hot corrosion tests, 75% wt.Na₂SO₄ and 25%wt. NaCl powders were selected as a corrosive salts. Samples were deposited with each of these salts until a total coating weight of 5 mg/cm² was reached according to **A.Anderson et. al procedure,2012**. The samples were measured and weighed first, then placed on a hot plated heated to 110°C. An air gun sprayed on the saturated aqueous –salt solutions in air mist and a coat of fine salt particles formed on the samples surfaces after the mist settled and the water evaporated. The process was repeated until the dry particles were deposited up to 5 mg/cm². Hot corrosion test was performed in a static air at (900°C) for 50 hr at 1 hr cycle in a programmable tube furnace. The experimental setup is shown in Figure 2 (University of Technology / Department of Production Engineering & Metallurgy). After testing the samples were cleaned in an ultrasonic bath, first in distilled water and then in ethanol. They were then weighed on a digital balance to determine the change in weight. The parabolic rate constant (Hot Corrosion Rate) K_p is calculated by a linear-square algorithm to a function in the form of $(\Delta W/A)^2 = K_p \times t$, where $\Delta W/A$ is the weight gain per unit surface area (mg/cm²) and t is the hot corrosion time in seconds.

4. EXPERIMENTAL DESIGN

Response surface methodology (RSM) is a technique that uses quantitative data from appropriate experiments to determine regression model equations and operating conditions. RSM is a collection of mathematical and statistical techniques for modeling and analysis of problems

in which a response of interest is influenced by several variables, **Douglas C.Montgomery,2009**. A standard RSM design called Box-Behnken Design (BBD) was applied in this work to study the variables for hot corrosion rate k_p ($10^{-12}g^2.cm^{-4}.s^{-1}$). BBD for three variables (wt.%Ce, wt.%Y, and wt.%Ge) each with two levels (the minimum and maximum), was used as experimental design model. The model has advantage that it permits the use of relatively few combinations of variables for determining the complex response function. A total of 15 experiments are needed to be conducted to determine 10 coefficients of second order polynomial, **Douglas C.Montgomery,2009**. In the experimental design model, wt.%Ce, wt.%Y, and wt.%Ge were taken as input variables. hot corrosion rate k_p ($10^{-12}g^2.cm^{-4}.s^{-1}$) was taken as the response of the system. The experimental design matrix derived from BBD is given in Table 2.

The output and input variables can be expressed as follow:

$$Y = f(X_1, X_2, X_3, X_4, \dots, X_n) \quad (1)$$

Where Y is the response of the system and X_i is the variables of action called factors where the goal is to optimize the response variable (Y). It is assumed that the independent variables are continuous and controllable by experiments with negligible errors. It is required to find a suitable approximation for the true functional relationship between independent variables and the response surfaces. The optimization of hot corrosion rate k_p ($10^{-12}g^2.cm^{-4}.s^{-1}$) was carried out by using Box-Behnken design with 12 unique runs including 3-replicates at center points. The quadratic equation model for predicting the optimal point was expressed according to Eq(2).

$$Y = \beta_0 + \sum_{i=1}^k \beta_i x_i + \sum_{i=1}^k \beta_{ii} x_i^2 + \left(\sum_{i=1}^{k-1} \sum_{j=i+1}^k \beta_{ij} x_i x_j \right)_{i < j} \quad (2)$$

Three factors were studied and their low and high levels are given in Table 3. hot corrosion rate k_p ($10^{-12}g^2.cm^{-4}.s^{-1}$) was studied with a standard RSM design called Box-Behnken Design (BBD). Fifteen experiments were conducted in duplicate according to the scheme mentioned in Table 2. Minitab and Matlab program was used for regression and graphical analysis of the data obtained. The optimum values of the selected variables were obtained by solving the regression equation and by analyzing the response surface contour plots. The variability in dependent variables was explained by the multiple coefficient of determination, R^2 which is can be calculated according to equation (3), where n is the number of data pairs, x is independent variable, and y is dependent variable. and the model equation was used to predict the optimum value and subsequently to elucidate the interaction between the factors within the specified range, **Douglas C.Montgomery,2009**.

$$R^2 = \left(\frac{n(\sum xy) - (\sum x)(\sum y)}{\sqrt{[n(\sum x^2) - (\sum x)^2][n(\sum y^2) - (\sum y)^2]}} \right)^2 \quad (3)$$

5. RESULTS AND DISCUSSIONS

The results of the each experiments are given in Table 2. Empirical relationships between the response and the independent variables have been expressed by the quadratic model as shown in Figure 3 . Regression coefficient of full polynomial model is also shown in this Figure .

Analysis of variance has been calculated to analyze the accessibility of the model. The analysis of variance for the response has been predicted in Figure 4 . In general, ANOVA table is used to evaluate the goodness of the model , as a rule , if p-value is less than 0.05, model parameter is significant . On the basis of analysis of variance, the conclusion is that the selected model adequately represents the data for hot corrosion rate k_p ($10^{-12}g^2.cm^{-4}.s^{-1}$) . The Experimental values and the predicted values are in perfect match with R^2 value of 0.983 (Figure 5) . This methodology could therefore be successfully employed to study the importance of main and interaction effects of the test variables in hot corrosion test

6. DEVELOPING THE ANN MODEL

Artificial neural network (ANN) is a network with nodes or neurons analogous to the biological neurons. The nodes are interconnected to the weighted links. The weights are adjustable and can be trained by learning and training process and training treatments. ANN is able to receive inputs patterns in order to produce a pattern on its outputs that are correct for that class i.e. The ANN modeling can be an excellent approach in simulating the out-put results, **Daniel Graupe, 2007**. The three variables (wt.%Ce, wt.%Y, and wt.%Ge) each play important roles in influencing hot corrosion properties like hot corrosion rate k_p ($10^{-12}g^2.cm^{-4}.s^{-1}$). The target of this research is to establish nonlinear relationships between the input parameters and the output parameters by the usage of ANN networks. So to model the hot corrosion kinetics, the three variables (wt.%Ce, wt.%Y, and wt.%Ge)has been defined as input and hot corrosion rate k_p ($10^{-12}g^2.cm^{-4}.s^{-1}$) as outputs in network. In this work, three input layers, ten hidden layers and one output layer, are used for predicting hot corrosion rate k_p ($10^{-12}g^2.cm^{-4}.s^{-1}$) according to Figure 6 . Sigmoid and pureline transfer function was employed for hidden layers and output layer, respectively. After neural networks are trained successfully, all output results is stored as shown in Figure 7. Figure 8 presents the comparison between measured and predicted results for hot corrosion rate k_p ($10^{-12}g^2.cm^{-4}.s^{-1}$). The agreements between the predicted and measured values ($R^2=0.94$) indicate that this approach can be very useful in modelling the hot corrosion properties of hot corrosion rate k_p ($10^{-12}g^2.cm^{-4}.s^{-1}$) in hot corrosion kinetics.

7. GENETIC ALGORITHM (GA)

The genetic algorithm approach provides the solution for the global optimization i.e. to find the "best possible" solution in decision models that frequently have a number of sub-optimal (local) solutions. The genetic algorithm solves optimization problems by mimicking the principles of biological evolution, repeatedly modifying a population of individual points using rules modelled on gene combinations in biological reproduction, **David A. Coley,1999**. Due to its random nature, the genetic algorithm improves the chances of finding a global solution. Thus

they prove to be very efficient and stable in searching for global optimum solutions. The mathematical model that best describes the relationship between Input and output parameters has to be developed in order to be used as objective function in GA to aid the global optimization. The Mathematical model was obtained using the Regression function in Minitab software. The proposed mathematical model was used to formulate the objective functions, which was the prerequisite of genetic algorithm. The objective function was solved using MATLAB software as shown in Figure 9. The optimized process parameter level of Genetic algorithm was obtained from this Figure. Figure 10 shows the plot of variation of hot corrosion rate k_p ($10^{-12} \text{g}^2 \cdot \text{cm}^{-4} \cdot \text{s}^{-1}$) with the number of generation which is obtained by MATLAB program. The initial variation in the curve is due to the search for optimum solution. It is evident that the minimum hot corrosion rate k_p ($10^{-12} \text{g}^2 \cdot \text{cm}^{-4} \cdot \text{s}^{-1}$) is 71.701.

The optimal values of input variables from regression equations using GA for the hot corrosion rate k_p ($10^{-12} \text{g}^2 \cdot \text{cm}^{-4} \cdot \text{s}^{-1}$) were shown in Table 4. The optimum values of weight percentages (Wt.%) of Ce, Y, and Ge from Box-Behnken design were found to be 3, 3 and 3 respectively. The minimum predicted value of hot corrosion rate k_p ($10^{-12} \text{g}^2 \cdot \text{cm}^{-4} \cdot \text{s}^{-1}$) was found to be 71.701.

The hot corrosion rate k_p ($10^{-12} \text{g}^2 \cdot \text{cm}^{-4} \cdot \text{s}^{-1}$) was studied by Wt.%Ce and Wt.%Y. The results have been depicted in Figure 11a. The results indicated that the minimum hot corrosion rate k_p ($10^{-12} \text{g}^2 \cdot \text{cm}^{-4} \cdot \text{s}^{-1}$) has been occurred in the 3wt.% Ce and 3wt.% Y. The combined effect of wt.%Ce and wt.%Ge has been presented in Figure 11b. The results show that the minimum hot corrosion rate k_p ($10^{-12} \text{g}^2 \cdot \text{cm}^{-4} \cdot \text{s}^{-1}$) was recorded at the 3wt.% Ce and 3wt.% Ge. In the same way, the effect of wt.%Y and wt.%Ge on the hot corrosion rate k_p ($10^{-12} \text{g}^2 \cdot \text{cm}^{-4} \cdot \text{s}^{-1}$), the minimum hot corrosion rate k_p ($10^{-12} \text{g}^2 \cdot \text{cm}^{-4} \cdot \text{s}^{-1}$) was 71.701 for 3wt.% Y and 3wt.% Ge as shown in Figure 11c.

The microstructure using optical microscope for coating (a) and hot corrosion (b) systems is shown in Figure 12. Figure 13 shows the EDAX (a), and XRD (b) analysis. These analyses show that the coated layer at the optimum conditions consists of Ce-Y-Ge doped (Al+Cr). The addition of Ce, Y, and Ge to the coated layer improve bond strength of the coatings to the substrate [14]. The formation of oxides of aluminum and chromium contribute to the development of hot corrosion resistance of this coating. XRD analysis indicate a scale consisting of a layer containing oxides of aluminum (Al_2O_3) and chromium (Cr_2O_3), thus Al-Cr diffusion coatings on Superfer 800H in molten salt environments at 900°C are found effective in decreasing corrosion rate in molten salt, due to the formation of protective oxide scales of Al_2O_3 and Cr_2O_3 .

8. CONFIRMATION TEST FOR GENETIC ALGORITHM

The confirmation test for Genetic algorithm approach at the optimized process parameter levels (3Wt.%Ce, 3Wt.%Y, 3Wt.%Ge) was done and the hot corrosion rate k_p ($10^{-12} \text{g}^2 \cdot \text{cm}^{-4} \cdot \text{s}^{-1}$) exhibited by the hot corrosion test of Superfer 800H was found to be $72.113 \times 10^{-12} \text{g}^2 \cdot \text{cm}^{-4} \cdot \text{s}^{-1}$ i.e. there is a good agreement between GA and experimental results.



9. CONCLUSIONS

The results obtained in this study lead to the following conclusions:

1. Response surface methodology using Box-Behnken design prove very effective model for studying the influence of wt.% of doping elements on hot corrosion rate .
2. The experimental values and predicted values are perfect match with R^2 value of 98.30 .
3. ANN model has been developed for predicting Kp as function of wt.% of doping elements (Ce,Y,Ge) . The model has been proved to be successful in terms of agreements with experimental results.
4. The developed GA model can be used to find the optimal wt.% of doping elements (Ce,Y,Ge) which minimize the hot corrosion rate during the hot corrosion tests . A confirmation experiment was also conducted and verified the effectiveness of GA method.
5. EDS and XRD reveal the presence of elements of mixture in coating layer and the formation of the dense and continuous protective Al_2O_3 and Cr_2O_3 scale on surface during hot corrosion tests .

REFERENCES

- Lin-Chang Tsai1, Hung-Hua Sheu, Cheng-Chieh Chen, Ming-Der Ger, *The Preparation of the Chromized Coatings on AISI 1045 Carbon Steel Plate with the Electroplating Pretreatment of Ni or Ni/Cr-C Film*, Int. J. Electrochem. Sci., 10 (2015) 317 – 331.
- Fahamsyah H. Latief, El-Sayed M. Sherif, Koji Kakehi, *Role of Aluminide Coating on Oxidation Resistance of Ni-Based Single Crystal Superalloy at 900 °C*, Int. J. Electrochem. Sci., 10 (2015) 1873 – 1882 .
- Subhash Kamal , Korada Viswanath Sharma , A. M. Abdul-Rani, *Hot Corrosion Behavior of Superalloy in Different Corrosive Environments*, Journal of Minerals and Materials Characterization and Engineering, 2015, 3, 26-36 .
- Subhash Kamal, R. Jayaganthan, S. Prakash , *High temperature cyclic oxidation and hot corrosion behaviours of superalloys at 900°C* , Bulletin of Materials Science, June 2010, Volume 33, Issue 3, pp 299-306 .
- T. S. Sidhu, S. Prakash and R. D. Agrawal , *Hot corrosion and performance of nickel-based coatings*, CURRENT SCIENCE, VOL. 90, NO. 1, 10 JANUARY 2006 , pp 41-47 .
- Marta Kianicova , Karel Slamecka , Jaroslav Pokluda , *Damage Of Diffusion Coatings On Turbine Blades*, Brno, Czech Republic, EU18. 2011,20- 5 .
- W.H Lee, R.Y Lin, *Hot corrosion mechanism of intermetallic compound Ni_3Al* , Materials Chemistry and Physics, Volume 77, Issue 1, 2 January 2003, Pages 86-96 .
- LIN Nai-ming, , XIE Fa-qin, ZHOU Jun, ZHONG Tao, WU Xiang-qing, TIAN Wei, *Microstructures and wear resistance of chromium coatings on P110 steel fabricated by pack cementation*, J. Cent. South Univ. Technol. (2010) 17: 1155–1162 .

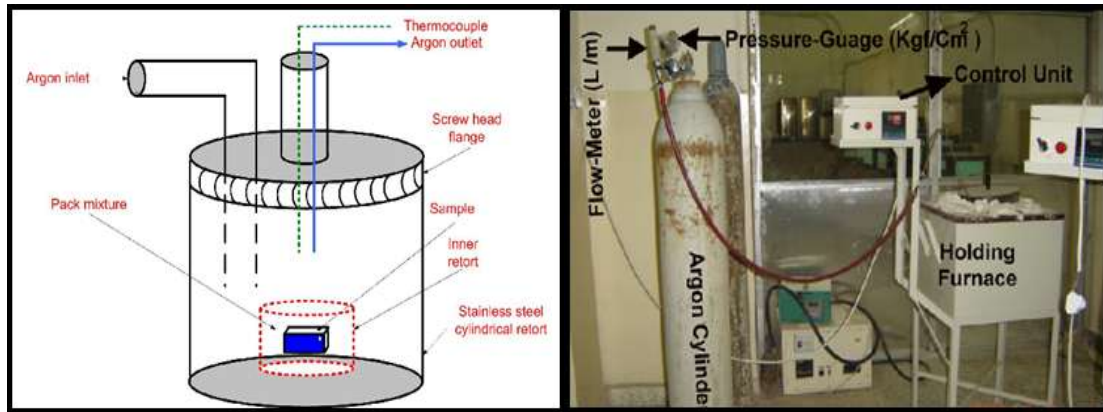


- Bruce M. Warnes, Nick S. DuShane, Jack E. Cockerill, *Cyclic oxidation of diffusion aluminide coatings on cobalt base superalloys*, Surface and Coatings Technology 148 (2001) 163–170.
- A. ESLAMI, H. ARABI and S. RASTEGARI, *Gas Phase Aluminizing Of A Nickel Base Superalloy By A Single Step Htha Aluminizing Process*, Canadian Metallurgical Quarterly, Vol 48, No 1., 2009, pp 91-98.
- I.M. Edmonds, H.E. Evans, C.N. Jones, *Oxidation & Coating Evolution In Aluminized Fourth Generation Bladealloys*, The mineral, metal materials society , superalloy2008, pp.661-670.
- H. R. Karimi Zarchi, M. Soltanieh, M. R. Aboutalebi, X. Guo, *Thermodynamic study on pack aluminizing systems of pure titanium and nickel* , Trans. Nonferrous Met. Soc. China 23(2013) 1838–1846 .
- Chao C. Jain and Chun H. Koo, *Creep and Corrosion Properties of the Extruded Magnesium Alloy Containing Rare Earth*, Materials Transactions, Vol. 48, No. 2 (2007) pp. 265 to 272.
- Rajesh Ranjan Sinha, Dr. Brahm Deo Tripathi, Dr. Mahendra Yadav, Mines, Dhanbad, *Effect of rare earth additions on high-temperature oxidation resistance of V and Mo alloyed steels*, steel-grips.com 2013,pp.14-18.
- Hongyu Wang , Dunwen Zuo, Gang Chen,, Guifang Sun , Xiangfeng Li,, Xu Cheng, *Hot corrosion behaviour of low Al NiCoCrAlY cladded coatings reinforced by nano-particles on a Ni-base super alloy*, Corrosion Science 52 (2010) 3561–3567.
- Rober A.Rapp, Mark A.Haper and Robert Bianco, *Codeposition elements by Halide Activated Pack Cementation*, JOM, Vol3, No.14,Nov.1991,pp.20-25.
- Anderson and S.Ramachandran, A. *Analysis of Corrosion at Hot Environment of Plasma Sprayed Stainless Steels* , European Journal of Scientific research, ISSN1450-216X Vol.76 No.2 (2012) , pp. 300-308.
- Douglas C.Montgomery , *Design and Analysis of Experiments*, John Wily &Sonc, Inc., 2009 .
- Daniel Graupe, *Principles Of Artificial Neural Networks*, 2nd Edition, World Scientific Publishing Co. Pte. Ltd., 2007.

- David A. Coley, *An Introduction to Genetic Algorithms for Scientists and Engineers*,World Scientific Publishing Co. Pte. Ltd.1999.

Table 1. Chemical composition of substrate material.

Element	Co	Cr	Ti	Al	W	Ta	C	B	Mo	Ni
Wt.%	8.4	16	3.31	3.23	1.07	0.59	0.13	0.05	1.02	bal



(a) Pack Cementation retort

(b) Pack Cementation Furnace

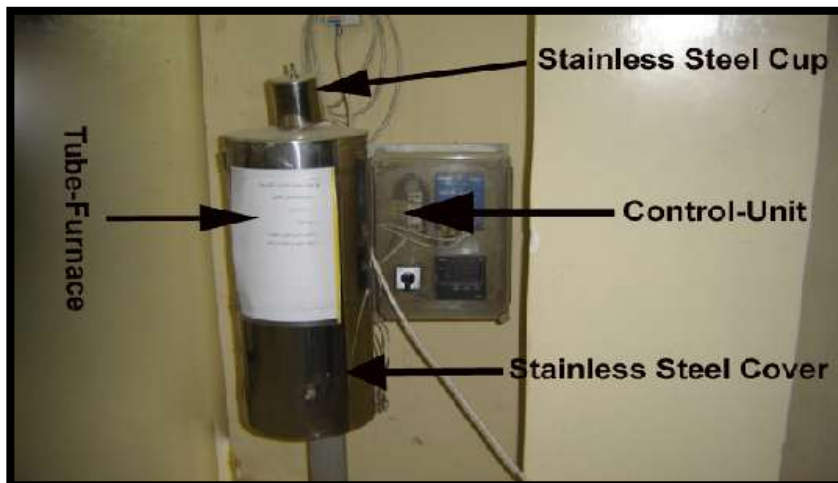
Figure 1. Apparatus used for pack cementation .**Figure 2.** A programmable tube furnace of hot corrosion test.



Table 2. Experimental design and results for hot corrosion rate k_p ($10^{-12} \text{g}^2 \cdot \text{cm}^{-4} \cdot \text{s}^{-1}$)

Run	Coded Values			Actual Values			k_p ($10^{-12} \text{g}^2 \cdot \text{cm}^{-4} \cdot \text{s}^{-1}$)	
	X ₁	X ₂	X ₃	X ₁	X ₂	X ₃	observed	Predicted
1	0	1	1	2	3	3	74.81	74.64
2	1	1	0	3	3	2	75.76	75.51
3	1	-1	0	3	1	2	77.65	77.46
4	0	1	-1	2	3	1	76.39	76.62
5	1	0	-1	3	2	1	80.55	80.57
6	-1	-1	0	1	1	2	81.19	81.44
7	-1	1	0	1	3	2	79.35	79.54
8	0	0	0	2	2	2	83.33	83.55
9	0	-1	-1	2	1	1	78.28	78.45
10	0	0	0	2	2	2	83.43	83.55
11	-1	0	1	1	2	3	82.7	82.68
12	1	0	1	3	2	3	77.04	77.46
13	-1	0	-1	1	2	1	83.76	83.34
14	0	-1	1	2	1	3	76.89	76.66
15	0	0	0	2	2	2	83.88	83.55

Table 3. Coded and actual values of variables of the experimental design

Factor		Coded levels of variables		
		-1	0	+1
Wt.%Ce	X ₁	1	2	3
Wt.%Y	X ₂	1	2	3
Wt.%Ge	X ₃	1	2	3

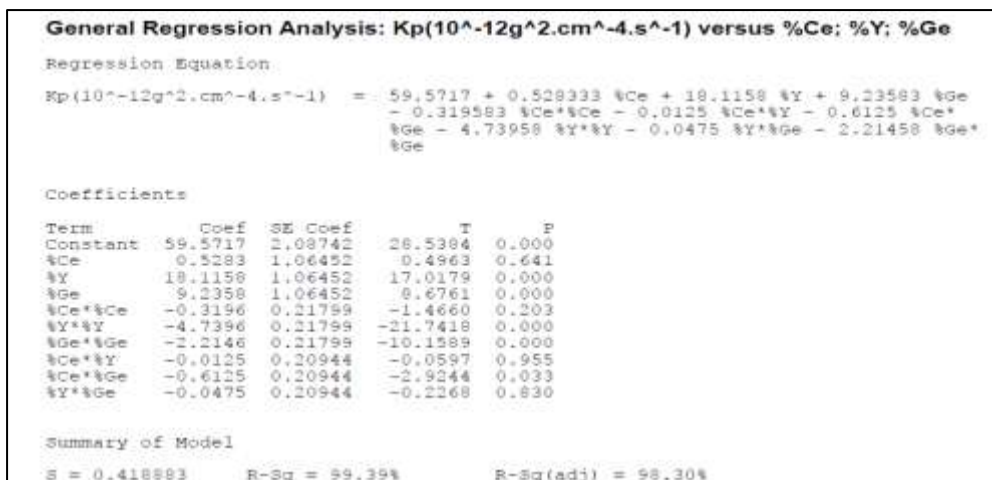


Figure 3. MINITAB session show the results of general regression.

Analysis of Variance						
Source	DF	Seq SS	Adj SS	Adj MS	F	P
Regression	9	143.800	143.800	15.9778	91.060	0.000053
Error	5	0.877	0.877	0.1755		
Total	14	144.677				

Figure 4. MINTAB session for ANOVA of regression model.

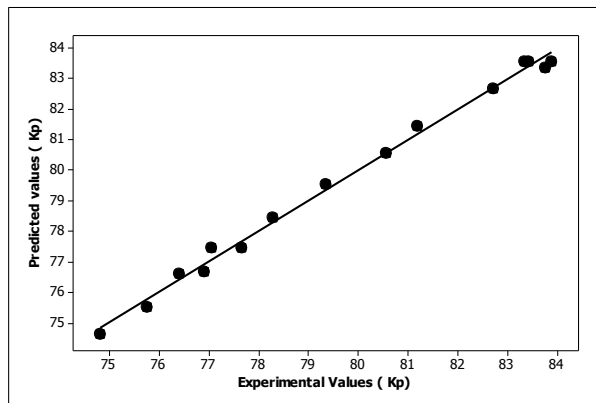


Figure 5. Comparison between predicted and experimental values.

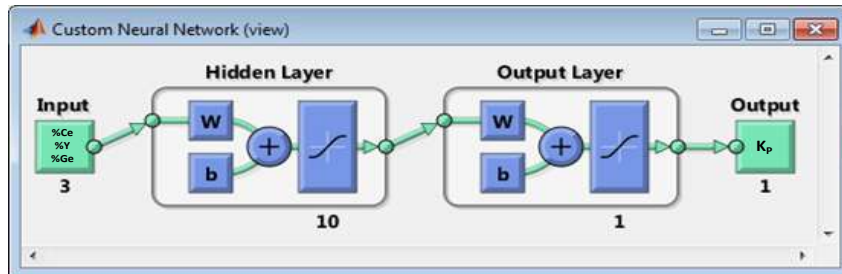


Figure 6. ANN Structure for input, hidden and output layers.

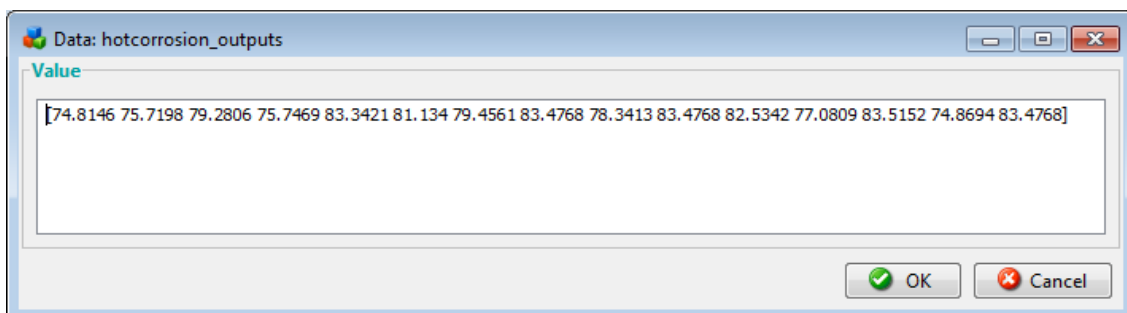


Figure 7. Results of ANN-outputs.

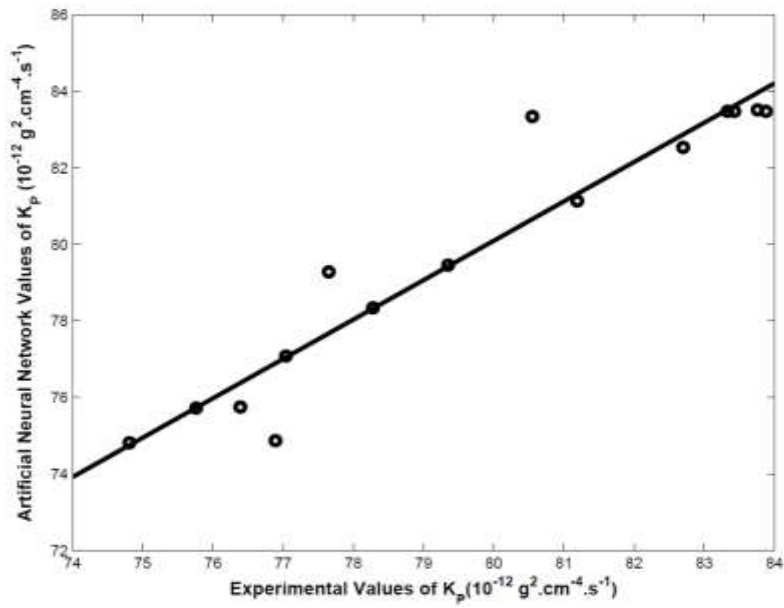


Figure 8. Comparison of the experimentation and calculation.

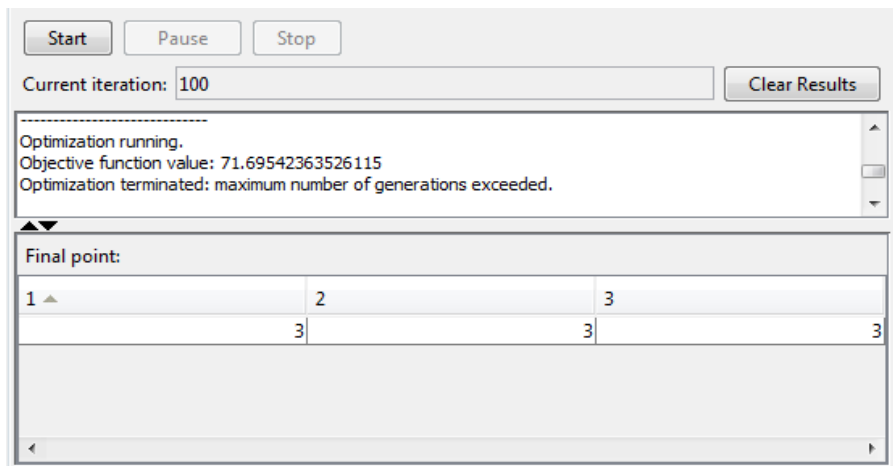


Figure 9. Solver showing the results in MATLAB.

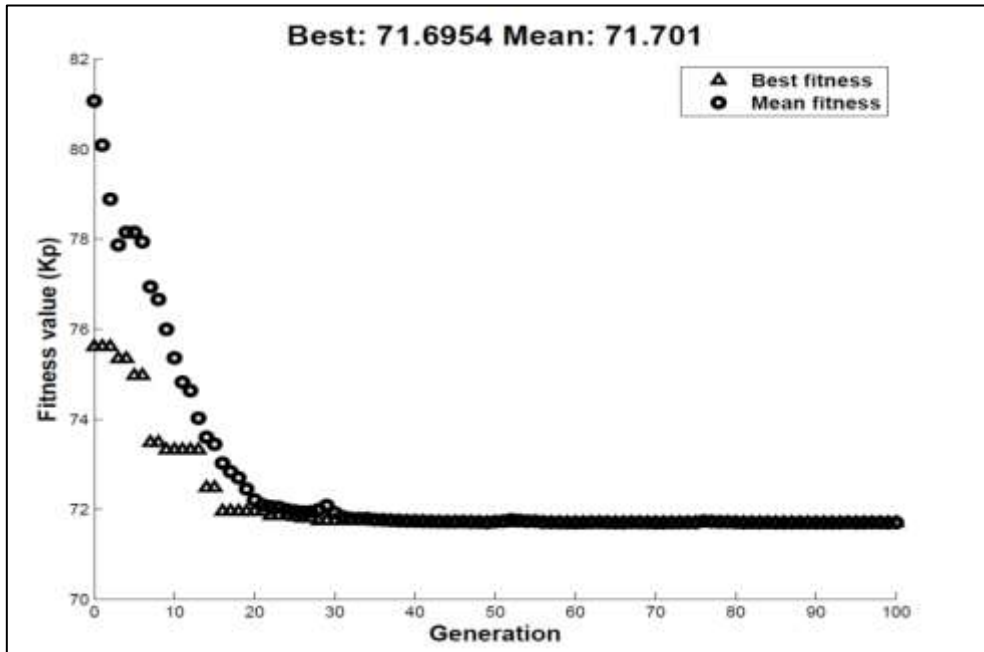


Figure 10. Variation of hot corrosion rate k_p ($10^{-12} \text{g}^2 \cdot \text{cm}^{-4} \cdot \text{s}^{-1}$) with number of generation.

Table 4. Optimum values of variable obtained from GA of regression model

No.	parameter	Optimum value	Minimum predicted k_p $10^{-12} \text{g}^2 \cdot \text{cm}^{-4} \cdot \text{s}^{-1}$
1	Wt.%Ce	3	71.701
2	Wt.%Y	3	
3	Wt.%Ge	3	

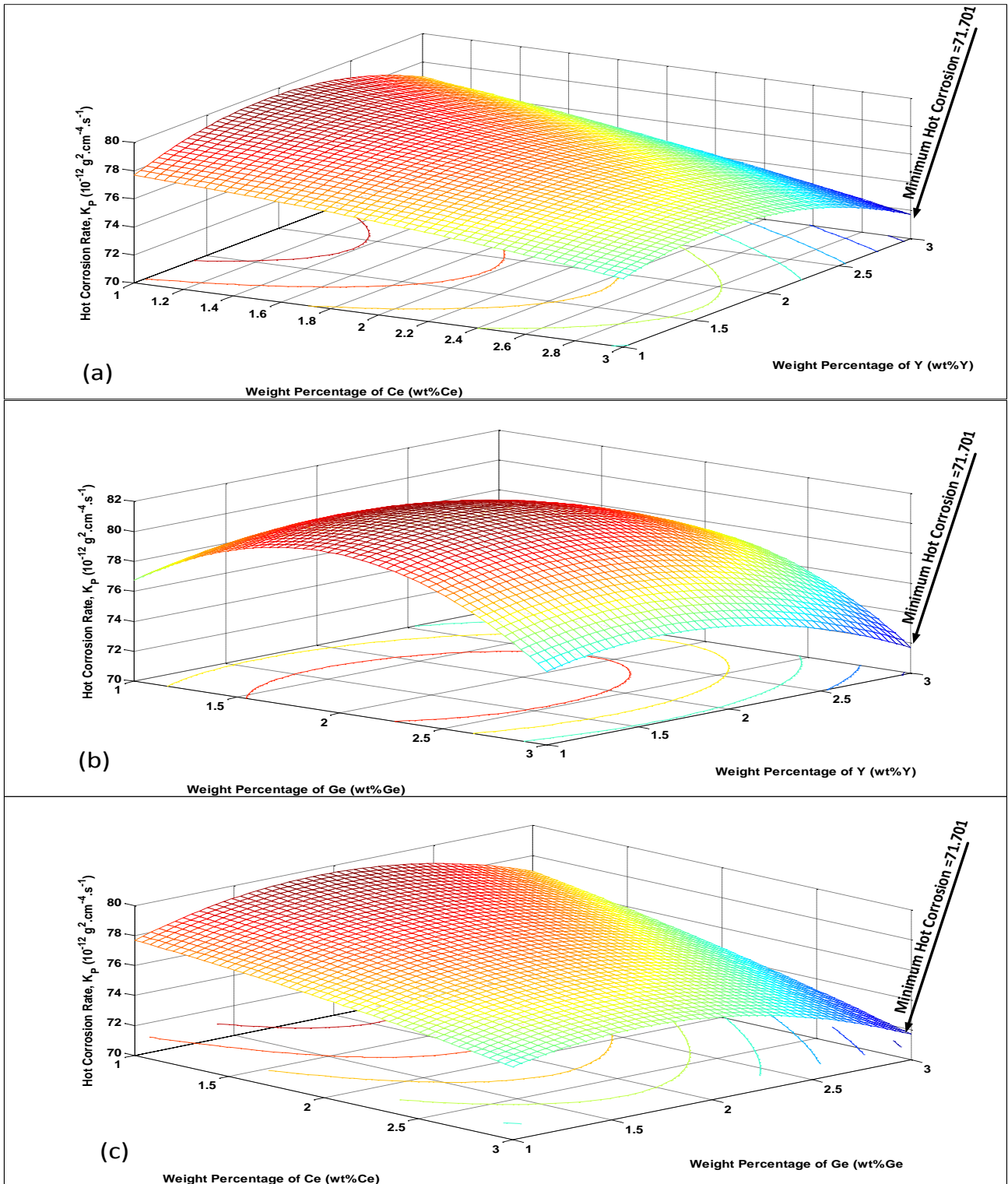


Figure 11. Response surface of 3D plot indicating the effect of interaction between (a) wt.%Ce and wt.%Y on hot corrosion rate k_p ($10^{-12} \text{ g}^2 \cdot \text{cm}^{-4} \cdot \text{s}^{-1}$) while holding wt.%Ge at 3wt.% (b) wt.%Ce and wt.%Ge on hot corrosion rate k_p ($10^{-12} \text{ g}^2 \cdot \text{cm}^{-4} \cdot \text{s}^{-1}$) while holding wt.%Y at 3wt.% (c) wt.%Y and wt.%Ge on hot corrosion rate k_p ($10^{-12} \text{ g}^2 \cdot \text{cm}^{-4} \cdot \text{s}^{-1}$) while holding wt.%Ce at 3wt.%

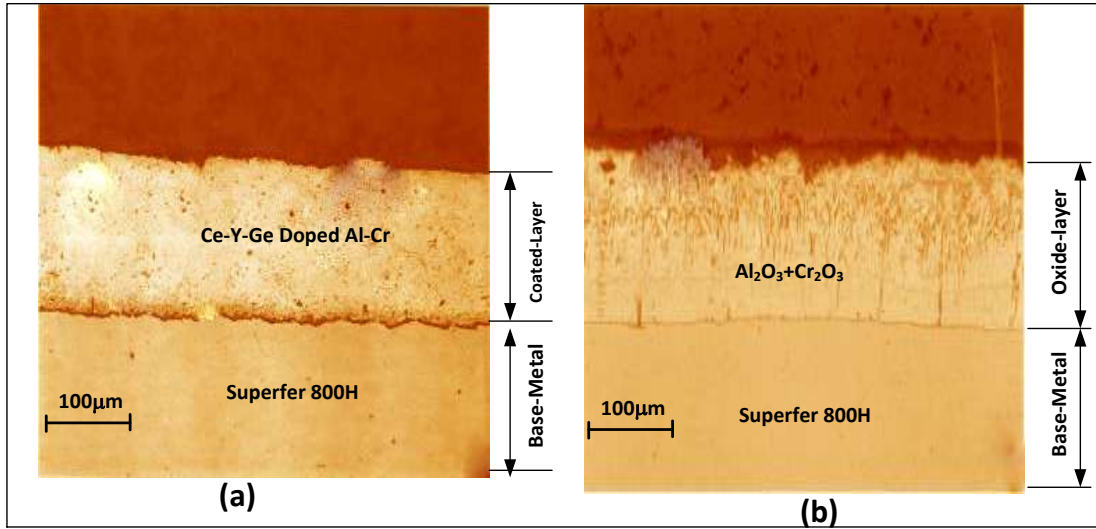


Figure 12. The microstructure using optical microscope for coating (a) and hot corrosion(b) systems

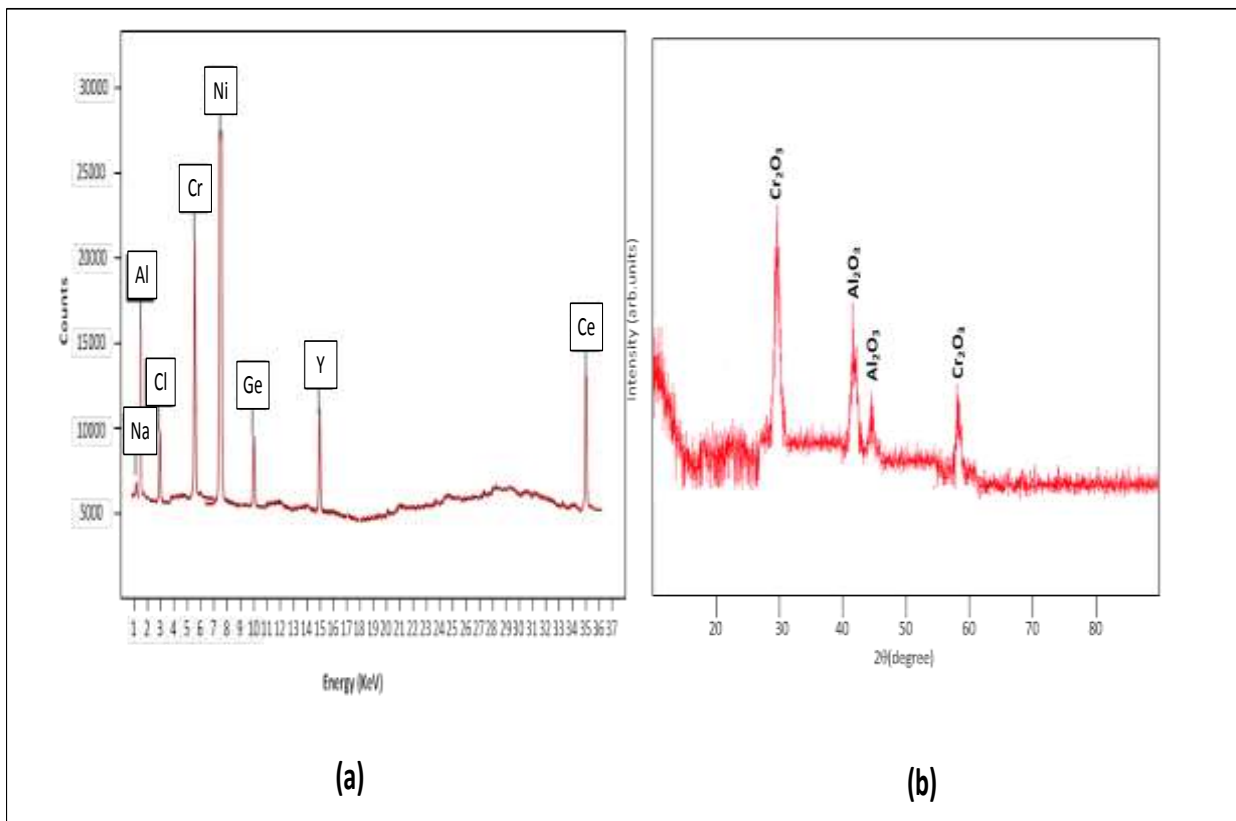


Figure 13. The EDAX (a), and XRD (b) analysis.